

# A Simple Parametrisation of the Pion Form Factor

Matthew Kirk,<sup>1,\*</sup> Bastian Kubis,<sup>2,†</sup> M  ril Reboud,<sup>3,‡</sup> and Danny van Dyk<sup>1,§</sup>

<sup>1</sup>*Institute for Particle Physics Phenomenology and Department of Physics, Durham University, Durham DH1 3LE, UK*

<sup>2</sup>*Helmholtz-Institut f  r Strahlen- und Kernphysik (Theorie) and*

*Bethe Center for Theoretical Physics, Universit  t Bonn, 53115 Bonn, Germany*

<sup>3</sup>*Universit   Paris-Saclay, CNRS/IN2P3, IJCLab, 91405 Orsay, France*

We discuss a novel and simple parametrisation of the pion vector form factor that transparently connects spacelike and timelike regions of the momentum transfer  $q^2$ . Our parametrisation employs the framework of conformal mapping and respects the known analyticity properties of the form factor, accounting explicitly for the  $\rho(770)$ -meson pole. The parametrisation manifestly fulfils the normalisation condition at  $q^2 = 0$  as well as further restrictions at the pion production threshold and in the limit  $|q^2| \rightarrow \infty$ . In contrast to the widely used Omn  s parametrisation, our approach does not use the pion–pion scattering phase shift as input. We confront the parametrisation with experimental data from  $\pi H$  scattering and  $\tau^- \rightarrow \pi^- \pi^0 \nu$  decay. We already find a good description of the data with only five free parameters, which include the pole mass and decay width of the  $\rho(770)$ .

## PRELIMINARIES

Hadronic form factors are scalar-valued functions that emerge in a variety of processes such as  $e^+e^- \rightarrow \pi\pi$ , or  $\bar{B} \rightarrow \pi\ell^-\bar{\nu}$ . They parametrise the mismatch between the partonic amplitude and the hadronic one, cannot be computed perturbatively, and commonly contribute substantially to the theory uncertainties in such processes.

We set out to use a series expansion approach to parametrise a hadronic form factor both below and above its respective pair production threshold, whilst fulfilling a dispersive bound. A past attempt at this idea was instructive but ultimately unsuccessful [1]. The salient difference between this past approach and our proposed parametrisation is our explicitly accounting for above-threshold poles on the 2nd Riemann sheet. In this, we make use of the analytic structure of the hadronic form factors as discussed in Ref. [2].

We start with summarizing the analytic structure of a generic hadronic form factor  $F(q^2)$  for two pseudoscalar mesons  $P_1$  and  $P_2$  with masses  $M_1$  and  $M_2$ , respectively, with  $M_1 \geq M_2$ ; see Ref. [3] for a textbook reference. This type of form factor emerges in the description of the semileptonic decay  $P_1 \rightarrow P_2 \bar{\ell}\ell'$ , and further processes related to this decay by crossing symmetry. In fact, the form factor describes the dynamics of the interaction of these mesons in three distinct regions of phase space *simultaneously*. First, it describes the scattering process  $P_1\ell \rightarrow P_2\ell'$  for  $q^2 \leq 0$ . Second, it describes the semileptonic decay  $P_1 \rightarrow P_2 \bar{\ell}\ell'$  for  $(m_\ell + m_{\ell'})^2 \leq q^2 \leq (M_1 - M_2)^2 \equiv t_-$ . Third, it describes the pair production process  $\ell\ell' \rightarrow \bar{P}_1 P_2$  for  $q^2 \geq t_+ \equiv (M_1 + M_2)^2$ . Here, we only consider a single form factor that is free of singularities to the left of  $t_-$ . We note at this point already that in this case, the overall phase of  $F$  can be chosen such that  $\arg F(q^2) = 0$  for  $q^2 \leq t_-$ . Hence, the form factor fulfils the Schwarz reflection condition, *i.e.*,  $F(q^2 + i\epsilon) = F^*(q^2 - i\epsilon)$  for

$q^2 \geq t_+$  and  $\text{Disc}_{q^2} F(q^2)$  is purely imaginary.

When parametrising the form factor for the scattering and decay regions of the phase space, one commonly uses a dispersively-bounded parametrisation of the form factor  $F(q^2)$  [4–6]:

$$F(q^2) = \frac{1}{\phi_F(q^2)P_{\text{sub}}(z(q^2))} \sum_{n=0}^{\infty} a_n z(q^2)^n. \quad (1)$$

Here  $z(q^2)$  represents a conformal mapping of the complex  $q^2$  plane to the open unit disk  $|z| < 1$ ,

$$z(q^2; t_+, t_0) = \frac{\sqrt{t_+ - q^2} - \sqrt{t_+ - t_0}}{\sqrt{t_+ - q^2} + \sqrt{t_+ - t_0}}, \quad (2)$$

where  $t_0$  is an arbitrary parameter  $-\infty < t_0 < t_+$  that can be chosen to improve the convergence of the sum in the parametrisation. Moreover,  $\phi_F$  represents the so-called outer function, which is fully determined in the construction of the dispersive bound, and  $P_{\text{sub}}$  represents the product of so-called Blaschke factors accounting for all below-threshold poles, *i.e.*, poles due to the presence of bound states with mass  $M$  where  $t_- < M^2 < t_+$ . The usage of Blaschke factors to account for the below-threshold poles ensures that  $|P_{\text{sub}}| = 1$  for  $t_+ \leq q^2$ . In the following, we assume the absence of below-threshold poles to streamline the notation — including such poles is a straightforward exercise. As a consequence, we use  $P_{\text{sub}} = 1$  from this point forward.

This form of parametrisation benefits from the presence of a dispersive bound

$$\begin{aligned} \int_{t_+}^{\infty} dq^2 \omega_F(q^2) |F(q^2)|^2 &= \frac{1}{2\pi} \oint \frac{dz}{iz} \left| \sum_{n=0}^{\infty} a_n z^n \right|^2 \\ &= \sum_{n=0}^{\infty} |a_n|^2 < 1. \end{aligned} \quad (3)$$

Here  $\omega_F(q^2)$  is determined in the derivation of the bound and positive definite on the support of the integral. Consequently,  $\phi_F$  is chosen to compensate for the presence of  $\omega_F$  and the Jacobian of the change of variable from  $q^2$  to  $z$ .

We show here that a parametrisation of the type shown in Eq. (1) can be extended into the pair production region of phase space ( $q^2 > t_+$ ) with a few modifications. Our new parametrisation ansatz takes the form

$$F(q^2) = \frac{W(z)}{\phi_F(z)} \frac{f(z)}{[z - z_r][z - z_r^*]} \Big|_{z=z(q^2)}, \quad (4)$$

with

$$f(z) = \sum_{n=0}^N b_n z^n. \quad (5)$$

The above differs from the common prescription in two aspects.

- First, a weight function  $W(z)$  is available to counteract the pathological behaviour of the outer function  $\phi_F$  in the timelike region at  $z \rightarrow \pm 1$ . This type of pathological behaviour has been previously discussed in Ref. [1] in the context of the timelike pion form factor and in Refs. [7, 8] in the context of the  $B \rightarrow \pi$  vector form factor. We further use  $W$  to manifestly ensure the correct asymptotic behaviour in the limit  $z \rightarrow 1$  (e.g.,  $F(q^2 \rightarrow \infty) \sim 1/q^2$ ).
- Second, the factor  $[z - z_r][z - z_r^*]$  in the denominator of Eq. (4) accounts for the presence of an above-threshold resonance  $r$  in the pair production process  $\ell\ell' \rightarrow r \rightarrow \bar{P}_1 P_2$ , with mass  $M_r$  and decay width  $\Gamma_r$ . This resonance gives rise to two complex-conjugate poles of the form factor  $F$  at  $z_r$  and  $z_r^*$  on its 2nd Riemann sheet [2]. The conformal mapping Eq. (2) maps the 2nd Riemann sheet onto the outside of the unit circle in  $z$ , yielding

$$1/z_r = z \left( (M_r - i\Gamma_r/2)^2 \right). \quad (6)$$

The above pole position fulfils  $|z_r| > 1$  and  $\text{Im } z_r < 0$ . The presence of two complex-conjugate poles is necessary to ensure that  $F$  fulfils the Schwarz reflection principle, i.e., that  $F$  is real-valued for  $q^2 \in \mathbb{R}$  with  $q^2 < t_+$  [2]. The generalisation of our ansatz to the case of multiple relevant above-threshold resonances is straightforward.

Despite our best efforts, we are currently not able to maintain the manifest orthogonality of the contributions to the saturation, i.e., the bound is not manifestly a sum of positive definite quantities.

We emphasise that the factor  $[z - z_r][z - z_r^*]$  introduced in Eq. (4) cannot — in general — be replaced by a

product of Blaschke factors for our purpose. The reason is that a Blaschke factor describing a pole on the 2nd Riemann sheet is always accompanied by a zero on the 1st Riemann sheet. However, a variety of form factors are known to exclude the presence of zeros on the first Riemann sheet; see, e.g., Refs. [9, 10] for the pion vector form factor. Hence, to leave sufficient flexibility in the parametrisation to avoid these additional zeros, we choose not to use Blaschke factors.

The convergence of a series expansion as shown in Eq. (4) is discussed in Ref. [1]. Due to the branch cut in  $q^2$ ,  $F$  is defined in the timelike region for momentum values with infinitesimal imaginary parts. The conformal mapping Eq. (2) maps these values to the inside of the unit disk, i.e., in the region of convergence of the series expansion. Abel's theorem further ensures that the series converges towards its value on the unit circle when it exists.

## APPLICATION TO THE PION FORM FACTOR

As a proof-of-concept analysis, we study the application of our parametrisation to  $F_\pi^{I=1}$ . In the isospin symmetry limit, this form factor corresponds to the isospin  $I = 1$  projection of the electromagnetic pion form factor  $F_\pi^{\text{e.m.}}$ . Limiting the analysis to  $F_\pi^{I=1}$  avoids the complexity of  $\rho$ - $\omega$  mixing [11, 12] and ensures the absence of poles due to  $I = 0$  resonances. The form factor  $F_\pi^{I=1}$  is defined by

$$(p_1 - p_2)^\mu F_\pi^{I=1}(q^2) = \frac{1}{\sqrt{2}} \langle \pi^-(p_1) \pi^0(p_2) | \bar{d}\gamma^\mu u | 0 \rangle, \quad (7)$$

where  $q^2 = (p_1 + p_2)^2$ . Our choice of this particular form factor is motivated by the fact that it is free of below-threshold poles and that ample experimental data is available to determine  $|F_\pi^{I=1}|^2$  both at timelike and at spacelike  $q^2$ . In this proof-of-concept study, we set out to describe the pion form factor up to  $\text{Re } q^2 \leq 1 \text{ GeV}^2$ . In this region, the  $I = 1$  form factor has a single resonance above threshold, which corresponds to the  $\rho(770)$  meson. We determine the pole mass and width of the  $\rho$  as part of our fit. Analyticity-based descriptions of the pion vector form factor (see, e.g., Refs. [9, 13–21]) are often based on the Omnès representation [22], which describes the elastic part of  $F_\pi^{I=1}$  in terms of the pion-pion  $P$ -wave phase shift  $\delta_1^1$ ,

$$\Omega(q^2) = \exp \left( \frac{q^2}{\pi} \int_{4M_\pi^2}^{\infty} dt \frac{\delta_1^1(t)}{t(t - q^2)} \right). \quad (8)$$

We do not use the phase as input here but rather check *a-posteriori* its consistency with studies of Roy equations [23–25], after fitting data on the form factor modulus. For dispersion relations reconstructing the form factor phase from its modulus, see Ref. [26] and references

therein. By construction, our parametrisation Eq. (4) fulfils Eq. (8) for  $\Omega = |F_\pi^{I=1}|$  and  $\delta_1^1 = \arg F_\pi^{I=1}$  for every choice of the truncation order  $N$ .

The outer function as shown in Eq. (16) exhibits zeros at  $z \rightarrow \pm 1$ , implying that  $F_\pi^{I=1} \sim 1/\phi_F$  diverges at  $z \rightarrow \pm 1$ . However,  $F_\pi^{I=1}$  is finite in both points. As discussed in Ref. [1], this implies that the weight function  $W$  should be chosen to manifestly remove these spurious divergences rather than letting the series expansion achieve this as part of the fit. Moreover, in the limit  $q^2 \rightarrow \infty$ , QCD imposes that  $F_\pi^{I=1}(q^2) \sim 1/q^2$  [27, 28] (up to logarithmic corrections), or equivalently  $F_\pi^{I=1}(q^2(z)) \sim (1-z)^2$ . We choose to manifestly impose this behaviour as part of the weight factor  $W$ . Hence, we partially follow Ref. [1] in using

$$W(z) = (1+z)^2(1-z)^{5/2}. \quad (9)$$

Armed with a model for the form factor  $F_\pi^{I=1}$ , we confront it with experimental data by performing a Bayesian fit using the EOS software [29] in version 1.0.13 [30]. Our choice of prior is defined as the product of independent uniform PDFs. For our nominal fit with truncation  $N =$ , we use the following prior intervals:

$$\begin{aligned} 0.757 \text{ GeV} &\leq M_\rho \leq 0.763 \text{ GeV}, \\ 0.141 \text{ GeV} &\leq \Gamma_\rho \leq 0.150 \text{ GeV}, \\ -0.08 &\leq b_2 \leq +0.08, \\ -0.09 &\leq b_3 \leq +0.09, \\ -0.05 &\leq b_4 \leq +0.07, \\ -0.02 &\leq b_5 \leq +0.02. \end{aligned} \quad (10)$$

This choice of prior contains more than 99% of the marginal posterior. Further fits are documented as part of the ancillary material [31]. We emphasise that the coefficients  $b_0$  and  $b_1$  are fixed by imposing  $F(q^2 = 0) = 1$  (due to charge conservation) and  $\text{Im} F(q^2 = t_+) \sim (q^2 - t_+)^{3/2}$  (due to angular momentum conservation). The latter is achieved by eliminating the term  $\text{Im} F(q^2 = t_+) \supset (q^2 - t_+)^{1/2}$ ; see Ref. [8] for a similar application for the  $B \rightarrow \pi$  form factor. Hence, a truncation at order  $N = 1$  corresponds to only two fit parameters: the mass  $M_\rho$  and the total decay width  $\Gamma_\rho$  of the  $\rho$  meson.

The likelihood is comprised of the product of individual, independent contributions:

**Belle:** The Belle experiment has determined  $|F_\pi^{I=1}|^2$  at timelike  $q^2$  from measurements of the decay  $\tau^- \rightarrow \pi^- \pi^0 \nu$  [33]. Here, we use the correlated measurements as a multivariate Gaussian likelihood, corresponding to 19 observations.

**CLEO:** The CLEO experiment has determined  $|F_\pi^{I=1}|^2$  at timelike  $q^2$  from measurements of the decay  $\tau^- \rightarrow \pi^- \pi^0 \nu$  [34]. Here, we use the correlated measurements as a multivariate Gaussian likelihood, corresponding to 29 observations.

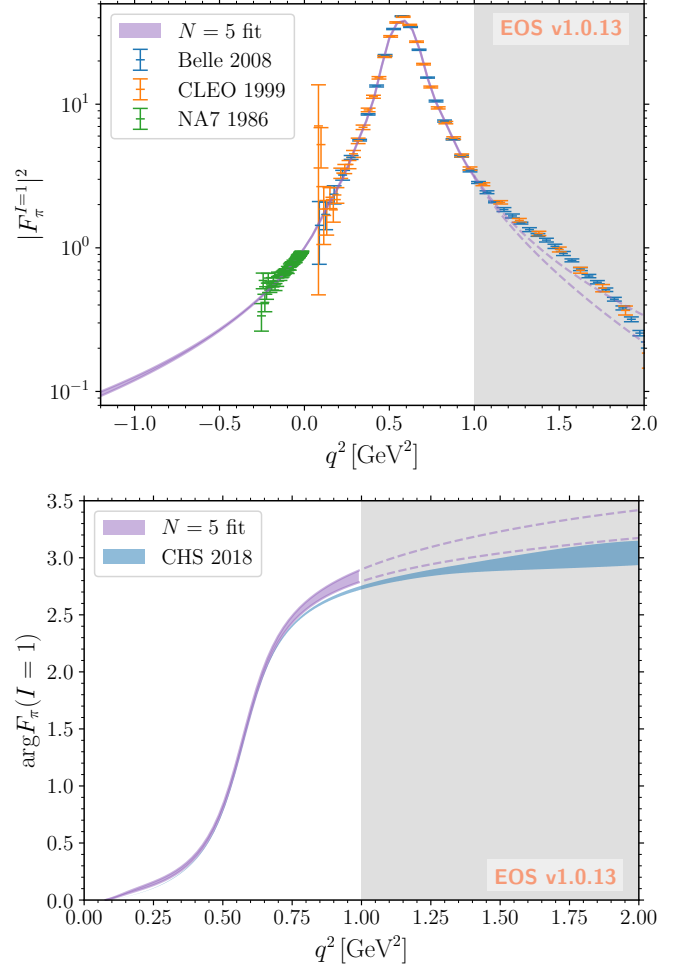


FIG. 1. The squared magnitude (top) and the phase (bottom) of the form factor  $F_\pi^{I=1}(q^2)$ . We show the envelope at 68% probability for truncation  $N = 5$  juxtaposed with data by the Belle, CLEO, and NA7 experiments. A single data point by the JLab- $F_\pi$  experiment at  $q^2 = -2.45 \text{ GeV}^2$  is not shown but agrees within  $0.8\sigma$  with the best-fit curve. Data points in the shaded region ( $q^2 \geq 1 \text{ GeV}^2$ ) are not fitted. However, we extend the posterior-prediction of the  $N = 5$  fit into this region as two dashed curves, indicating only the 68% envelope. For reference, we overlay our phase predictions with the input from Ref. [32].

**NA7:** The NA7 experiment has used  $\pi H$  scattering to determine  $|F_\pi^{\text{e.m.}}|^2$  at spacelike  $q^2$  [35].<sup>1</sup> Here, we assume the data points to be uncorrelated in their statistical error and fully positively correlated in their systematical error. We use the NA7 results at spacelike  $q^2$  as a multivariate Gaussian likelihood,

<sup>1</sup> The NA7 experiment extracts from their data the electromagnetic form factor  $F_\pi^{\text{e.m.}}$ , which differs from the  $I = 1$  projection by an isospin-symmetry-violating term  $F_\pi^{I=0}$ . For this work, the latter is assumed to be small in the spacelike region. A simultaneous analysis of both isospin projections is left for future work.

truncation $N$	$\chi^2$	d.o.f.	$p$ value [%]	$\langle r_\pi^2 \rangle$ [fm <sup>2</sup> ]	$M_\rho$ [MeV]	$\Gamma_\rho$ [MeV]	bound saturation
1	$\approx 3300$	92	$< 10^{-10}$	—	—	—	0.46
2	$\approx 1500$	91	$< 10^{-10}$	—	—	—	0.44
3	117.4	90	2.8	$0.474 \pm 0.0022$	$760.4 \pm 0.4$	$143.0 \pm 0.6$	0.46
4	98.17	89	23.8	$0.457 \pm 0.0045$	$760.2 \pm 0.4$	$145.9 \pm 0.9$	0.46
5	97.9	88	22.1	$0.460 \pm 0.0061$	$760.0 \pm 0.6$	$146.1 \pm 0.9$	0.46

TABLE I. Goodness-of-fit diagnostics for the fits with truncation  $N = 1$  through  $N = 5$  along-side postdictions of pion charge radius  $r_\pi^2$  and the  $\rho$  pole mass & decay width as well as saturation of the dispersive bound.

corresponding to 45 observations.

**JLab- $F_\pi$ :** The JLab- $F_\pi$  experiment has used pion electroproduction to determine  $F_\pi^{\text{e.m.}}$  at spacelike  $q^2 = -2.45 \text{ GeV}^2$ , amongst others [36, 37] (see Footnote 1). We use this single data point due to its large leverage, *i.e.*, the largest magnitude in  $q^2$  available to use experimentally. Other data points at  $q^2 = -1.6 \text{ GeV}^2$  [36] and in the interval  $q^2 \in [-2.45, -0.6] \text{ GeV}^2$  [37] are also obtained; however, the correlation between the various data points is not clear to us. Since the 2nd data point is found to be well compatible with our nominal fit, we conservatively use the  $q^2 = -2.45 \text{ GeV}^2$  data point only, corresponding to 1 observation.

Therefore our fits feature in total  $94 - (N + 1)$  degrees of freedom. We consider any given truncation order to describe the available data well if the corresponding  $p$  value exceeds 3%.

We carry out a series of fits for truncation orders  $N = 1$  through  $N = 5$ . The quality of these fits is evidenced by Table I, together with the predicted pion radius, the  $\rho$  resonance parameters, and the saturations of the dispersive bound that we computed numerically from the left-hand-side integral in Eq. (3).

We find that already for  $N = 1$ , the parametrisation visually describes the salient features of the available data. For the fits with  $N = 1$  to  $N = 3$ , we find  $p$  values below our a-priori threshold. For  $N = 4$ , we obtain a  $p$  value of  $\sim 20\%$ , indicating that the parametrisation starts to describe the data sufficiently well. Switching from  $N = 4$  to  $N = 5$ , the  $p$  value does not increase, leading us to adopt the  $N = 5$  fit as our nominal fit, which is shown in Fig. 1. We further find that the  $N = 5$  best-fit point is compatible with the  $N = 4$  best-fit point, with the additional parameter  $b_5^{N=5}$  compatible with zero within its uncertainties.

We note in passing that a fit to only the data in the timelike region yields an excellent description of that data but suffers from a multimodal posterior, with the individual modes corresponding to solutions with a different number of zeros on the first Riemann sheet. Using the data in the spacelike region eliminates all but one of the modes, which corresponds to the absence of any zeros of

$F_\pi^{I=1}$  on the 1st Riemann sheet.

Our nominal predictions for the  $\rho$  resonance parameters show perfect agreement and smaller uncertainties than the previous pole determinations [24, 38, 39], which are summarised as  $M_\rho \in [761, 765] \text{ MeV}$  and  $\Gamma_\rho \in [142, 148]$  in the world average [40]. Our nominal result for the pion charge radius  $\langle r_\pi^2 \rangle = 0.460(6) \text{ fm}^2$  shows a puzzling tension with the results in the literature [32, 40, 41]. In addition, we find a systematic deviation between the argument of the form factor determined from our fit and the determinations in the literature [32]. These differences motivate a more systematic study of our approach with respect to the potential impact of further poles and inelastic contributions, which is left to future work.

We find the saturation of the dispersive bound to be in good qualitative agreement with previous results on the saturation [42].

## CONCLUSION

We have presented a simple parametrisation of hadronic form factors with above-threshold poles. Crucially, our proposed parametrisation does not require the  $\pi\pi$  scattering phase shift as an input, unlike Omnès-based parametrisations. We use our proposed parametrisation to fit the isospin-one projection of the pion vector form factor as a first application. Already at low truncation order  $N = 4$ , *i.e.*, using  $M_\rho$ ,  $\Gamma_\rho$  and only three independent shape parameters, we find an excellent description of the experimental data for  $q^2 \leq 1 \text{ GeV}^2$ . We provide posterior predictions of the phase of the form factor as an auxiliary result. We look forward to promising future applications, such as a simultaneous analysis of the isospin-one and isospin-zero projections of the pion form factor including the  $\omega$  resonance, or an extension of our current work to higher resonances. Due to the universality of the final-state interactions, we also envisage the wider application of our approach to hadronic form factors for flavour-changing currents, such as in  $\bar{B} \rightarrow \pi\pi\ell^-\bar{\nu}$  transitions.

## ACKNOWLEDGEMENTS

We are grateful to Florian Herren for valuable discussions and comments on the manuscript. DvD is grateful to Martin Jung for valuable discussions on a precursor to this analysis. BK and DvD gratefully acknowledge past support by the DFG through the funds provided to the Sino—German Collaborative Research Center TRR110 “Symmetries and the Emergence of Structure in QCD” (DFG Project-ID 196253076 – TRR 110). DvD acknowledges ongoing support by the UK Science and Technology Facilities Council (grant numbers ST/V003941/1 and ST/X003167/1).

## Relation to the $\rho$ Coupling Constants

Close to the  $\rho$  resonance, the  $\rho\pi\pi$  and  $\rho\gamma$  interactions are described by the Lagrangian [43]

$$\mathcal{L}_\rho \supset g_{\rho\pi\pi} \epsilon^{abc} \pi^a \partial^\mu \pi^b \rho_\mu^c - \frac{eM_\rho^2}{g_{\rho\gamma}} A^\mu \rho_\mu. \quad (11)$$

In the vicinity of the pole  $s_\rho = (M_\rho - i\Gamma_\rho/2)^2$ , the form-factor  $F_\pi$  can be related to these couplings through its residue on the second Riemann sheet [2, 43]

$$\text{Res}(F_{\pi,\text{II}}, s_\rho) = -\frac{s_\rho g_{\rho\pi\pi}}{g_{\rho\gamma}} \quad (12)$$

Analyticity and elastic unitarity imply further that the value on the first Riemann sheet is related to the  $\rho$  couplings as well [2, 43]

$$F_{\pi,\text{I}}(s_\rho) = -\frac{24i\pi}{g_{\rho\pi\pi}g_{\rho\gamma}} \left(1 - \frac{4M_\pi^2}{s_\rho}\right)^{-3/2}. \quad (13)$$

As a consequence, our simple analysis of the pion form factors provides full access to both couplings simultaneously. This is a great advantage over the more involved methods based on the Roy equations, see, *e.g.*, Ref. [44]. From our nominal fit model, we determine

$$\begin{aligned} g_{\rho\pi\pi} &= 6.09(6) - 0.3(1)i = 6.10(6)e^{-0.05(2)i} \\ g_{\rho\gamma} &= 4.87(1) - 0.17(2)i = 4.87(2)e^{-0.035(4)i}, \end{aligned} \quad (14)$$

in good agreement with the literature.

## Outer Function

The outer function for the pion vector form factor reads [1]

$$\begin{aligned} \phi_F(q^2; t_0) &= \sqrt{\frac{1}{48\pi\chi}} \left(\frac{t_+ - q^2}{t_+ - t_0}\right)^{\frac{1}{4}} \\ &\quad \left(\sqrt{t_+ - q^2} + \sqrt{t_+ - t_0}\right) (t_+ - t)^{\frac{3}{4}} \\ &\quad \left(\sqrt{t_+ - q^2} + \sqrt{t_+}\right)^{-\frac{1}{2}} \left(\sqrt{t_+ - q^2} + \sqrt{t_+ + Q^2}\right)^{-3}, \end{aligned} \quad (15)$$

where  $t_+ = (M_{\pi^+} + M_{\pi^0})^2$  is the threshold,  $-\infty < t_0 < t_+$  is a free parameter in the conformal mapping Eq. (2), and  $\chi = \chi(Q^2) = 6.839 \cdot 10^{-3} \text{ GeV}^{-2}$  incorporates the normalisation of the dispersive integral that gives rise to a bound of the type Eq. (3). This normalisation is obtained through a perturbative calculation of a suitable two-point function at a subtraction point  $Q^2$  [1] (see also Ref. [45] for a Lattice QCD estimate). We choose  $Q^2 = -t_0 = 1 \text{ GeV}^2$  for the purpose of this analysis. The outer function is more conveniently evaluated in terms of  $z$  rather than  $q^2$ :

$$\begin{aligned} \phi_F(z) &= (1+z)^2(1-z)^{1/2} \frac{1}{\sqrt{12\pi t_+ \chi}} \left(1 - \frac{t_0}{t_+}\right)^{5/4} \\ &\quad \left[\sqrt{1 - \frac{t_0}{t_+}}(1+z) + (1-z)\right]^{-1/2} \\ &\quad \times \left[\sqrt{1 + \frac{Q^2}{t_+}}(1-z) + \sqrt{1 - \frac{t_0}{t_+}}(1+z)\right]^{-3}. \end{aligned} \quad (16)$$

---

\* matthew.j.kirk@durham.ac.uk

† kubis@hiskp.uni-bonn.de

‡ merilreboud@gmail.com

§ danny.van.dyk@gmail.com

- [1] W. W. Buck and R. F. Lebed, New constraints on dispersive form-factor parameterizations from the time-like region, *Phys. Rev. D* **58**, 056001 (1998), arXiv:hep-ph/9802369.
- [2] I. Caprini, B. Grinstein, and R. F. Lebed, Model-independent constraints on hadronic form factors with above-threshold poles, *Phys. Rev. D* **96**, 036015 (2017), arXiv:1705.02368 [hep-ph].
- [3] I. Caprini, *Functional Analysis and Optimization Methods in Hadron Physics*, SpringerBriefs in Physics (Springer, 2019).
- [4] S. Okubo, Exact bounds for  $K_{l3}$  decay parameters, *Phys. Rev. D* **3**, 2807 (1971).
- [5] C. G. Boyd, B. Grinstein, and R. F. Lebed, Constraints on form-factors for exclusive semileptonic heavy to light meson decays, *Phys. Rev. Lett.* **74**, 4603 (1995), arXiv:hep-ph/9412324.

- [6] I. Caprini, L. Lellouch, and M. Neubert, Dispersive bounds on the shape of  $\bar{B} \rightarrow D^{(*)} \ell^- \bar{\nu}$  form-factors, Nucl. Phys. B **530**, 153 (1998), arXiv:hep-ph/9712417.
- [7] T. Becher and R. J. Hill, Comment on form-factor shape and extraction of  $|V_{ub}|$  from  $B \rightarrow \pi \ell \nu$ , Phys. Lett. B **633**, 61 (2006), arXiv:hep-ph/0509090.
- [8] C. Bourrely, I. Caprini, and L. Lellouch, Model-independent description of  $B \rightarrow \pi \ell \nu$  decays and a determination of  $|V_{ub}|$ , Phys. Rev. D **79**, 013008 (2009), [Erratum: Phys.Rev.D 82, 099902 (2010)], arXiv:0807.2722 [hep-ph].
- [9] H. Leutwyler, Electromagnetic form-factor of the pion, in *Continuous Advances in QCD 2002 / ARKADYFEST (honoring the 60th birthday of Prof. Arkady Vainshtein)* (2002) pp. 23–40, arXiv:hep-ph/0212324.
- [10] B. Ananthanarayan, I. Caprini, and I. S. Imsong, Implications of the recent high statistics determination of the pion electromagnetic form factor in the timelike region, Phys. Rev. D **83**, 096002 (2011), arXiv:1102.3299 [hep-ph].
- [11] S. Holz, C. Hanhart, M. Hoferichter, and B. Kubis, A dispersive analysis of  $\eta' \rightarrow \pi^+ \pi^- \gamma$  and  $\eta' \rightarrow \ell^+ \ell^- \gamma$ , Eur. Phys. J. C **82**, 434 (2022), [Addendum: Eur. Phys. J. C **82**, 1159 (2022)], arXiv:2202.05846 [hep-ph].
- [12] G. Colangelo, M. Hoferichter, B. Kubis, and P. Stoffer, Isospin-breaking effects in the two-pion contribution to hadronic vacuum polarization, JHEP **10**, 032, arXiv:2208.08993 [hep-ph].
- [13] I. Caprini, Dispersive and chiral symmetry constraints on the light meson form-factors, Eur. Phys. J. C **13**, 471 (2000), arXiv:hep-ph/9907227.
- [14] J. F. de Trocóniz and F. J. Ynduráin, Precision determination of the pion form-factor and calculation of the muon  $g - 2$ , Phys. Rev. D **65**, 093001 (2002), arXiv:hep-ph/0106025.
- [15] G. Colangelo, Hadronic contributions to  $a_\mu$  below one GeV, Nucl. Phys. B Proc. Suppl. **131**, 185 (2004), arXiv:hep-ph/0312017.
- [16] J. F. de Trocóniz and F. J. Ynduráin, The Hadronic contributions to the anomalous magnetic moment of the muon, Phys. Rev. D **71**, 073008 (2005), arXiv:hep-ph/0402285.
- [17] C. Hanhart, A New Parameterization for the Pion Vector Form Factor, Phys. Lett. B **715**, 170 (2012), arXiv:1203.6839 [hep-ph].
- [18] B. Ananthanarayan, I. Caprini, D. Das, and I. Sentitemsu Imsong, Two-pion low-energy contribution to the muon  $g - 2$  with improved precision from analyticity and unitarity, Phys. Rev. D **89**, 036007 (2014), arXiv:1312.5849 [hep-ph].
- [19] B. Ananthanarayan, I. Caprini, D. Das, and I. Sentitemsu Imsong, Precise determination of the low-energy hadronic contribution to the muon  $g - 2$  from analyticity and unitarity: An improved analysis, Phys. Rev. D **93**, 116007 (2016), arXiv:1605.00202 [hep-ph].
- [20] C. Hanhart, S. Holz, B. Kubis, A. Kupść, A. Wirzba, and C.-W. Xiao, The branching ratio  $\omega \rightarrow \pi^+ \pi^-$  revisited, Eur. Phys. J. C **77**, 98 (2017), [Erratum: Eur. Phys. J. C **78**, 450 (2018)], arXiv:1611.09359 [hep-ph].
- [21] B. Ananthanarayan, I. Caprini, and D. Das, Pion electromagnetic form factor at high precision with implications to  $a_\mu^{\pi\pi}$  and the onset of perturbative QCD, Phys. Rev. D **98**, 114015 (2018), arXiv:1810.09265 [hep-ph].
- [22] R. Omnès, On the Solution of certain singular integral equations of quantum field theory, Nuovo Cim. **8**, 316 (1958).
- [23] B. Ananthanarayan, G. Colangelo, J. Gasser, and H. Leutwyler, Roy equation analysis of  $\pi\pi$  scattering, Phys. Rept. **353**, 207 (2001), arXiv:hep-ph/0005297.
- [24] G. Colangelo, J. Gasser, and H. Leutwyler,  $\pi\pi$  scattering, Nucl. Phys. B **603**, 125 (2001), arXiv:hep-ph/0103088.
- [25] R. García-Martín, R. Kamiński, J. R. Peláez, J. Ruiz de Elvira, and F. J. Ynduráin, The Pion-pion scattering amplitude. IV: Improved analysis with once subtracted Roy-like equations up to 1100 MeV, Phys. Rev. D **83**, 074004 (2011), arXiv:1102.2183 [hep-ph].
- [26] E. Ruiz Arriola and P. Sánchez-Puertas, Phase of the electromagnetic form factor of the pion, Phys. Rev. D **110**, 054003 (2024), arXiv:2403.07121 [hep-ph].
- [27] G. P. Lepage and S. J. Brodsky, Exclusive Processes in Quantum Chromodynamics: Evolution Equations for Hadronic Wave Functions and the Form-Factors of Mesons, Phys. Lett. B **87**, 359 (1979).
- [28] G. R. Farrar and D. R. Jackson, The Pion Form-Factor, Phys. Rev. Lett. **43**, 246 (1979).
- [29] D. van Dyk *et al.* (EOS Authors), EOS: a software for flavor physics phenomenology, Eur. Phys. J. C **82**, 569 (2022), arXiv:2111.15428 [hep-ph].
- [30] D. van Dyk, M. Reboud, N. Gubernari, P. Lüghausen, D. Leljak, M. Kirk, S. Kürten, A. Kokulu, C. Bolognani, L. Gaertner, S. Meiser, V. Kuschke, F. Novak, C. Bobeth, F. Herren, E. Graverini, E. McPartland, M. Ritter, T. Blake, K. K. Vos, M. Bordone, E. Eberhard, E. Romero, I. Toijala, F. Beaujean, J. Eschle, M. Burgos, M. Rahimi, and R. O'Connor, textttEOS version 1.0.13 (2024).
- [31] M. Kirk, B. Kubis, M. Reboud, and D. van Dyk, EOS/DATA-2024-02: Supplementary material for EOS/ANALYSIS-2024-02, 10.5281/zenodo.13946874 (2024).
- [32] G. Colangelo, M. Hoferichter, and P. Stoffer, Two-pion contribution to hadronic vacuum polarization, JHEP **02**, 006, arXiv:1810.00007 [hep-ph].
- [33] M. Fujikawa *et al.* (Belle), High-Statistics Study of the  $\tau^- \rightarrow \pi^- \pi^0 \nu_{\tau}$  Decay, Phys. Rev. D **78**, 072006 (2008), arXiv:0805.3773 [hep-ex].
- [34] S. Anderson *et al.* (CLEO), Hadronic structure in the decay  $\tau^- \rightarrow \pi^- \pi^0 \nu_\tau$ , Phys. Rev. D **61**, 112002 (2000), arXiv:hep-ex/9910046.
- [35] S. R. Amendolia *et al.* (NA7), A Measurement of the Space-Like Pion Electromagnetic Form Factor, Nucl. Phys. B **277**, 168 (1986).
- [36] T. Horn *et al.* (Jefferson Lab  $F_\pi$ ), Determination of the Charged Pion Form Factor at  $Q^2 = 1.60$  and  $2.45$  (GeV/c)<sup>2</sup>, Phys. Rev. Lett. **97**, 192001 (2006), arXiv:nucl-ex/0607005.
- [37] G. M. Huber *et al.* (Jefferson Lab), Charged pion form-factor between  $Q^2 = 0.60$  GeV<sup>2</sup> and  $2.45$  GeV<sup>2</sup>. II. Determination of, and results for, the pion form-factor, Phys. Rev. C **78**, 045203 (2008), arXiv:0809.3052 [nucl-ex].
- [38] R. García-Martín, R. Kamiński, J. R. Peláez, and J. Ruiz de Elvira, Precise determination of the  $f_0(600)$  and  $f_0(980)$  pole parameters from a dispersive data analysis, Phys. Rev. Lett. **107**, 072001 (2011), arXiv:1107.1635 [hep-ph].
- [39] J. R. Peláez, Light scalars as tetraquarks or two-meson states from large  $N_c$  and unitarized chiral perturbation

- theory, *Mod. Phys. Lett. A* **19**, 2879 (2004), arXiv:hep-ph/0411107.
- [40] S. Navas *et al.* (Particle Data Group), Review of particle physics, *Phys. Rev. D* **110**, 030001 (2024).
  - [41] B. Ananthanarayan, I. Caprini, and D. Das, Electromagnetic charge radius of the pion at high precision, *Phys. Rev. Lett.* **119**, 132002 (2017), arXiv:1706.04020 [hep-ph].
  - [42] B. Ananthanarayan, I. Caprini, and B. Kubis, Constraints on the  $\omega\pi$  form factor from analyticity and unitarity, *Eur. Phys. J. C* **74**, 3209 (2014), arXiv:1410.6276 [hep-ph].
  - [43] M. Hoferichter, B. Kubis, and M. Zanke, Radiative resonance couplings in  $\gamma\pi \rightarrow \pi\pi$ , *Phys. Rev. D* **96**, 114016 (2017), arXiv:1710.00824 [hep-ph].
  - [44] M. Hoferichter, J. Ruiz de Elvira, B. Kubis, and U.-G. Meißner, Nucleon resonance parameters from Roy–Steiner equations, *Phys. Lett. B* **853**, 138698 (2024), arXiv:2312.15015 [hep-ph].
  - [45] S. Simula and L. Vittorio, Dispersive analysis of the experimental data on the electromagnetic form factor of charged pions at spacelike momenta, *Phys. Rev. D* **108**, 094013 (2023), arXiv:2309.02135 [hep-ph].